El Cezeri
Journal of Science and Engineering
ISSN: 2148-3736

Research Paper

Analysis of Boundary Layer Thickness and Temperature Distribution in a Fluidic Stream across a Stretching Sheet with Thermal Nonequilibrium and Viscous Heating Effects

Uchenna Awucha Uka[1a], Edwin Esekhaigbe[2b], Obi Boniface Inalu[3c]

[1]Basic Sciences Department, School of Science and Technology, Babcock University, Ogun State, Nigeria.
[2]Mathematics and Computer Science Department, University of Africa, Bayelsa State, Nigeria.
[3]Mathematics Department, Imo State University, Owerri, Nigeria.

ukau@babcock.edu.ng
DOI : 10.31202/ecjse.1513483
Received: 09.07.2024 Accepted: 28.03.2025
How to cite this article:
Uchenna Awucha Uka, Edwin Esekhaigbe, Obi Boniface Inalu, “Analysis of Boundary Layer Thickness and Temperature Distribution in a Fluidic Stream across a Stretching Sheet with Thermal Nonequilibrium and Viscous Heating Effects", El-Cezeri Journal of Science and Engineering, Vol: 12, Iss: 2, (2025), pp.(134-152).
ORCID: [a]0000-0003-4177-3213; [b]0009-0007-5337-0856, [c]0000-0002-4878-3994.

Abstract : The analysis of a boundary layer thickness and temperature distribution effects in a viscous fluid flow of varying Hartmann intensity and thermal nonequilibrium over an exponentially extending/attenuation sheet is discussed. The fundamental approach to the investigation includes the application of the similarity estimation scheme in the recovery of the ordinary differential equations (ODEs) from the governing partial differential equations (PDEs) of the conservation of momentum, energy, and mass concentration which were modeled from the Navier-Stokes equation. The recovered coupled ordinary differential equations (CODEs) were analytically solved using the series technique and evaluated numerically using the MATHEMATICA scheme. Furthermore, the effect of several physical parameters on the velocity, temperature, and concentration are investigated, presented in graphical forms, and carefully analyzed. Correspondingly, the impact of some parameters on the local Nusselt number and coefficient of skin friction was presented, tabulated, and discussed clearly. Notedly, it is found that as the Hartmann parameter improves, the drag and fluid velocity decrease. Additionally, the enhancement of the thermal nonequilibrium number led to a rise in the temperature. Also, a reduction in skin friction resulted from enhancing the threshold thermal Grashoff number. Equally, the local Nusselt number declines due to the surge in the Prandtl and thermal nonequilibrium parameters, respectively.

Keywords: Heat transfer, Thermal Gradient, Mass diffusivity, Hydromagnetic, Drag.

1. Introduction

Understanding the fluid dynamics past a stretched surface is crucial because of its wide range of applications. For example, sheets of metal and polymer are used in the fabrication of materials in many industrial and manufacturing processes. Its significance also ranges from the cooling of an immeasurable metallic plate in a cooling steam bath to paper manufacturing, glass blowing, steel revolving, and plastic film drawing. Sakiadis [1] explored the effect of the incompressible boundary layer drift of a flat material in motion. The impact of varying fluid characteristics on heat transfer and hydro-magnetic flow across a nonlinearly widening material has been examined by Poply et al. [2]. The problem was solved quantitatively. Prasad et al. [3] investigated the effects of temperature-dependent fluid characteristics on magnetohydrodynamic (MHD) natural stream flow and thermal movement past a nonlinearly strained sheet. They considered the effects of both the magnetic field and Prandtl numbers and used the Keller-Box technique to solve the problem numerically. It was found that the temperature increases as the magnetic strength improves. However, Renuka et al. [4] studied the MHD boundary layer flow influenced by radiation and mass transfer from an exponentially elongating surface due to the heat generation utilizing the Runge-Kuta fourth-order and shooting schemes. The influence of both the magnetic and heat source parameters was discussed. It was found that as the magnetic field intensity increases, the momentum boundary layer thickness shrinks while the temperature and concentration boundary layer thicknesses increase. The slip effect on the MHD boundary layer stream over an exponentially expanding plate with thermal radiation, suction, and blowing has been examined by Mukhopadhyay [5]. The result indicated that the temperature increases as a result of the enhancement of the thermal radiation and effective thermal diffusivity. The exploration of an MHD boundary layer flow of a viscid incompressible fluid movement across an exponentially enlarged sheet with the thermal radiation effect incorporated into the energy equation has been studied analytically by Mabood et al. [6]. The problem was solved using the homotopy analysis method (HAM). The result showed that the friction factor rises as the magnetic field increases. Poornima and Bhaskar [7] explored the impact of radiation on the MHD nanofluid with natural convective boundary wall drift across a nonlinear stretching sheet using the fourth-order Runge-Kutta and shooting methods. It was noted that the surge in the magnetic strength suppressed the velocity distribution. The non-aligned MHD inactive point flow of a flexible viscous nanofluid across a stretching sheet with radiation influence was presented by Khan et al. [8]. They discovered that as the magnetic constraint rises, the reattached non-alignment point diminishes.

The study of electrically conducting fluid dynamics in an electromagnetic field is known as magnetohydrodynamics (MHD). It is an important aspect of the modern metallurgical and metalworking processes. Thus, the constant dual-dimensional stagnation-point flow of a water-based nanofluid past an exponentially enlarging/lessening material in its plane has been investigated by Bachok et al. [9]. The numerical approach was used to investigate the three different forms of nanoparticles in the water-based fluid containing the Prandtl number. ($\mathbf{Pr = 6.2}$), copper ($\mathbf{Cu}$), alumina ($\mathbf{Al2O3}$), and titania ($\mathbf{TiO2}$). It was found that the shrinking sheet solution remains unexceptional. However, the similarity solution of a Casson nanofluid's heat transfer and steady boundary layer flow across a vertical cylinder expanding exponentially in its radial direction with the Prand, magnetic, Casson, and mixed convective effects has been explored according to Malik [10]. The equations obtained were solved using the Runge–Kutta Fehlberg approach and the result indicated that as the mixed convective parameter grows, so does the velocity. Eid [11] studied the impact of a chemical reaction on the MHD boundary layer flow of a two-phased nanofluid across an exponentially extending sheet. It was discovered that the source and reaction parameters affected the thermal boundary layer. Similarly, by using the Keller-Box approach, Gangaiah et al. [12] explored the MHD flow of a nanofluid over an exponentially stretched sheet with viscous dissipation and chemical reaction effects. Abel et al. [13] examined the numerical effect of several variables, such as the variable buoyancy, viscosity, and thermal conductivity on the mixed convective thermal transference over an exponentially stretched sheet. The Runge–Kutta Fehlberg and effective shooting methods were deployed in recovering the solution. Yousif et al. [14] utilized the shooting method with the fourth-order Runge-Kutta approach to scrutinize the numerical analysis of the momentum and heat transport of an MHD Carreau nanofluidic across an exponentially strained plate with an internal heat generation/absorption and radiation impact in the absence of the non-thermal equilibrium.

The basic phenomenon behind the dynamics of MHD is that the applied magnetic field drives the current and its effect produces the Lorentz force which impacts the fluid motion dramatically. Meanwhile, several MHD electrically conducting fluids such as plasma, electrolytes, liquid metals, etc., can be mathematically formulated using the Navier-Stokes equations. Hence, the study of MHD fluid remains a subject of significant research due to its vast application to several industrial processes such as the processing of magnetic materials and the generation of MHD electrical power. Additionally, it is useful in the fields of geophysics and astrophysics, radio transmission, solar structure, flow meters, and extraction of geothermal energy. Using the Runge–Kutta and shooting approaches, Ellahi et al. [15] studied the thermally charged MHD bi-phased flow coatings along slippery walls with non-Newtonian nanofluid and hafnium particles. It was observed that the improvement of the Brinkman number led to an increase in the temperature. The unsteady flow and heat transfer of a carbon nanotube-based (CNT) MHD nanofluid with varying viscosity over a permeable shrinking surface has been numerically explored by Ahmed et al. [16] through the application of the Keller-Box approach in the absence of both the Schmidt and Brinkman numbers. The results suggested that an increase in the suction parameter and shrinking magnitude led to an upsurge in the pressure profile. The problem of the tangent hyperbolic liquid stream past an exponentially changing upright cylinder has been reported by Naseer et al. [17]. The Runge-Kutta Fehlberg technique was used in solving the equations. Thus, the result indicated that the heat conductance of the fluid varies with temperature. By deploying the Keller-Box scheme, Rangi and Ahmad [18] examined the flow of a viscous fluid over a stretching cylinder in the presence of a variable thermal conductance. It was concluded that the temperature field is greatly impacted by the varying thermal conductivity. Similarly, Abel and Mathesha [19] studied the effects of temperature-dependent thermal conductivity, non-uniform heating, and thermal radiation on the MHD viscoelastic fluid flow across a stretched surface. The result affirmed that the temperature profile rises with varying thermal conductivity. However, Öztürk et al. [20] reported the presence of ideal constraints influencing thermal pipes' heating effectiveness via experimentation and the response wall approach with various forms of nanofluids within the heat exchangers. However, four parameters affecting the thermal efficiency were tested at three different levels of the experimental design. The analysis of variance (ANOVA) was used to test the model's accuracy. The ideal parameters were determined to be $\mathbf{SiO_2}$ nanoparticle concentration of $\mathbf{0.32}\%$ at the evaporator inlet temperature of $\mathbf{90}^\circ\mathbf{C}$ and a condenser Reynolds number of $\mathbf{21600}$. Öztürk et al. [21] adopted the Taguchi approach to investigate the effective improvement of the factors impacting the thermal efficiency of heated pipes with various types of nanofluids in the heat exchangers. The L27(3^4) orthogonal served as the basis for the experimental design at three levels for four parameters affecting the thermal efficiency with isopropyl alcohol as the basic fluid in the nanofluid suspension. Different quantities of silicon dioxide ($\mathbf{SiO_2}$), titanium dioxide ($\mathbf{TiO_2}$), and aluminum oxide $\mathbf{Al_2O_3}$ were tested at $\mathbf{0.2\ to\ 0.4\ at\ 0.6}\%$. The ideal parameters that were found using the analysis of variance (ANOVA) to assess the model's accuracy were the nanoparticle of the $\mathbf{SiO_2}$ concentration of $\mathbf{0.4}$, an evaporator inlet temperature of $\mathbf{80}^\circ\mathbf{C}$, and condenser air velocity of $\mathbf{1.2\ m/s}$.

The examination of the boundary layer flow of a viscous incompressible fluid over a nonlinear porous stretching sheet in the presence of a partial slip has been addressed by Mukhopadhyay [22]. The problem was numerically solved via the shooting method. It was observed that the horizontal velocity diminishes as the slip parameter increases. The existence of a dual solution for MHD boundary layer flow over a stretching/shrinking surface in the presence of thermal radiation and porous media was demonstrated by Rizwan et al. [23] through the aid of a KKL nanofluid model and Maple software. The result indicated that the fluid velocity in the upper branch rises as the magnetic parameter M increases while the fluid velocity in the lower branch decreases as M rises. Also, with the rising of the Biot number, the temperature profile improves on both the lower and upper branches. Furthermore, the influence of suction/injection on the local Nusselt number and the upper branch decreased as the magnetic parameter changed. The analysis of a boundary layer of a Jeffrey fluid flow across an expanding or contracting sheet past a porous medium has been examined by Nagaraju et al. [24]. The shooting and Runge-Kutta 4th-order approaches were deployed to derive the numerical solutions. The findings indicated that a rise in the heat source/sink causes a decline in the heat transfer rate. It was also found that an increase in thermal stratification enhances both the fluid temperature and velocity. Additionally, increasing the Jeffrey parameter decreases velocity and thickens the boundary layer. Shree et al. [25] analyzed the MHD boundary layer viscous flow past a stretching sheet by defining suitable non-dimensional parameters governing the boundary layer equations from the Falkner–Skan equations into a dimension-free form using the Legendre wavelet technique. The findings suggested that the thickness of the boundary layer diminishes as the pressure gradient and magnetic field parameters increase. Joseph et al. [26] explored the ımpact of the Brınkman and magnetıc fıeld numbers on a lamınar flow ın an upright channel. The single-term perturbation series approach was adopted to solve the modified equations. The findings showed that the magnetic field influences the velocity by diminishing turbulence and the Brinkmann number enhances the temperature distribution.

Despite all the aforementioned studies, the MHD boundary layer flow analysis of temperature distribution in a fluid across a stretched/shrunk plate with applied Hartmann, Brinkman, and Schmidt numbers has not received much attention. Inspired by this fact and its numerous significances in the areas of engineering, material science, manufacturing processes, and chemical applications a mathematical model for the boundary layer flow that represents the continuity, and conservation of momentum, energy, and mass equations is formulated. The similarity transformation and series schemes are applied to recover and solve the reformed coupled ordinary differential equations (RCODE) analytically. The results are graphically presented with legends, and the research findings are explained in detail.

However, the MHD effect plays a significant role in altering the boundary layer characteristics of a fluid as it flows over a stretching sheet, particularly in the presence of a magnetic field. The interaction between the motion of the fluid and the magnetic field can lead to changes in the momentum and thermal boundary layers thereby affecting both the momentum and thermal boundary layer thicknesses. Specifically, the impact of MHD tends to increase the boundary layer thickness due to the Lorentz force acting against the flow which counteracts the inertial effects of the fluid motion. As a result of this, the velocity gradient at the surface becomes less steep, leading to a broader region of slower movement of the fluid. Additionally, the presence of a magnetic field can enhance heat transfer mechanisms through the generation of eddies and vortices but may also compound thermal instability, particularly in higher temperature gradients where the uneven distribution of thermal energy can lead to fluctuations in the boundary layer distributions.

The thermal instability and viscous heating significantly influence the behavior of the boundary layer and temperature distribution. The viscous heating that arises from the internal friction as the fluid flows, tends to increase the fluid temperature thereby modifying the thermal boundary layer. This interaction may exacerbate the thermal stability of the fluid particularly when considering the influence of the thermal non-equilibrium which occurs when the temperatures of the fluid and stretching sheet are not consistent. Thus, this study focuses on these intricate dynamics in addressing how the MHD, thermal instability, and viscous heating collectively influence the boundary layer thickness and temperature distribution in a fluid flow. By incorporating these factors into a comprehensive model, the research fills the critical gap in understanding the interplay of these forces thereby yielding insights into the optimization of cooling rates and heat transfer in engineering applications such as material processing and thermal management in MHD systems. This approach enhances theoretical comprehension and provides practical advantages for improved design and greater efficiency in related industrial processes. This study makes a significant and original contribution by developing a comprehensive analytical and numerical framework to investigate the effects of varying Hartmann intensity and thermal nonequilibrium on viscous fluid flow over an exponentially stretching or attenuating sheet. The ordinary differential equations have been successfully derived through a similarity estimation method which streamlines the examination of the intricacies in fluid dynamics. The findings provide valuable insights into the interplay between fluid velocity, drag, and temperature distribution. It also reveals the critical relationship between the Hartmann and thermal Grashoff numbers. This research does not enhance the theoretical understanding of the boundary layer phenomena under thermal nonequilibrium conditions only but also validates its results with existing literature which illustrates high agreement with established literature.

Significantly, this study contributes to the existing literature by providing a comprehensive mathematical model that elucidates the complex interactions between boundary layer behavior and thermal dynamics in fluid flows over-stretching sheets. By addressing the impacts of thermal nonequilibrium and viscous heating, the research enhances the understanding of heat transfer mechanisms in several areas of applications such as polymer processing and cooling systems where precise thermal control is crucial. This work offers not just a detailed insight into the boundary layer characteristics and temperature distributions but also lays the groundwork for the development of more efficient cooling technologies and materials processing techniques. In a nutshell, this work augments the existing literature by addressing specific phenomena in fluid dynamics by providing new analytical techniques and results that contribute to the theoretical understanding and practical applications of fluid mechanics as well as thermal control. This study addresses a critical knowledge gap in understanding how combined MHD effects, thermal instability, and viscous heating influence the fluid dynamics in the boundary layers. While previous research has explored these phenomena in isolation, the present study integrates them into a comprehensive framework that captures their interdependencies and collective impact on both the boundary layer thickness and temperature distribution. Through the examination of these interactions in the thermal nonequilibrium conditions, the research yields important insights into the complex behavior of fluids and provides a more comprehensive understanding that is crucial in the design and enhancement of several industrial processes such as the thermal management and material processing. This comprehensive method not only enriches theoretical frameworks but also has real-world implications for increasing efficiency in applications to stretching sheets and magnetohydrodynamic systems.

3. Mathematical Formulation and Method

3.1. Materials

A two-dimensional steady incompressible and conducting viscous fluid over a stretched sheet in an applied magnetic field is considered. In the transverse direction to the wall of the stretching sheet, the fluid passes through an even magnetic field intensity B_o. Meanwhile, the $y-axis$ is normal to the sheet with the sheet positioned along the $x-axis$ at $y=0$. Since the induced magnetic field is insignificant due to the specified modest magnetic Reynolds number $(Re \ll 1)$, the applied magnetic field is being considered. However, both T_s and T_∞ are the wall and ambient temperatures while C_s and C_∞ are the concentrations of the sheet and the immediate vicinity of the sheet. Consequently, the following assumptions have been drawn.

- **Steady State Flow:** The flow is stable which implies that it is independent of time. Therefore, the momentum, conservation of energy, and concentration equations are steady and not functions of time.
- **Boundary Layer Approximation:** Since the problem involves a stretching sheet, it is likely for a boundary layer to be formed along the sheet. This suggests that the flow can be analyzed using the boundary layer theory since the variations in the flow properties are significant only in the vicinity of the sheet and can be neglected far from it.
- **Negligible Induced Magnetic Field:** Given that the magnetic Reynolds number is much less than 1 $(\mathrm{Re} \ll 1)$, the induced magnetic field due to the motion of the conducting fluid is negligible. This means that the primary magnetic field strength $(\mathrm{B_o})$ applied parallel to the surface of the sheet is considered in the present analysis.
- A constant pressure is incorporated.

Thus, the flow structure is shown below.

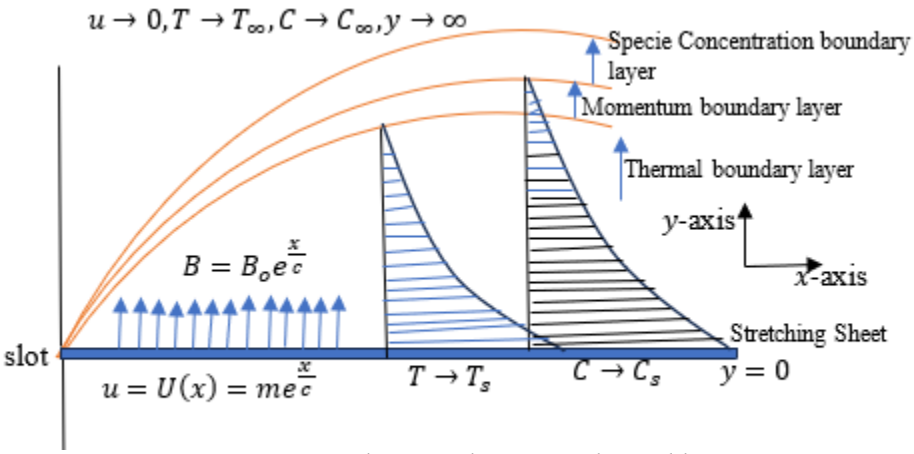

Figure 1. Schematic diagram of the problem

In terms of the modified Buongiorno's model [27], the reformed boundary layer mathematical equations of the flow are expressed as follows:

Continuity Equation

$$\frac{\partial u}{\partial x} + \frac{\partial v}{\partial y} = 0 \tag{1}$$

Momentum Equation

$$\frac{\partial p}{\partial x} + u\frac{\partial u}{\partial x} + v\frac{\partial u}{\partial y} = \mu\frac{\partial^2 u}{\partial y^2} + \frac{\sigma Bo^2 u}{\rho} + g\lambda\frac{T-T_\infty}{Re^2 x} \tag{2}$$

Energy Conservation Equation

$$u\frac{\partial T}{\partial x} + v\frac{\partial T}{\partial y} = \frac{K}{\rho cp} - \frac{\partial^2 T}{\partial y^2} + \frac{\mu}{\rho c_p}\left(\frac{T-T_\infty}{T_s-T_\infty}\right) \tag{3}$$

Mass Conservation Equation

$$u\frac{\partial C}{\partial x} + v\frac{\partial C}{\partial y} = \frac{\partial}{\partial y}(D_c)\frac{\partial C}{\partial y} \tag{4}$$

Subject to the boundary conditions

$$\begin{array}{ll} u = U_w(x) = me^{\frac{x}{c}},\ v = -v(x),\ T = T_s,\ C = C_s & \text{at } y = 0 \\ u \to 0,\ T \to T_\infty,\ C \to C_\infty & \text{as as } y \to \infty \end{array} \tag{5}$$

With the similarity transformation variables defined as

$$\eta = \sqrt{\frac{m}{2vc}}\, ye^{\frac{x}{2c}}\ , \Psi = f(\eta)\sqrt{2vcm}\, e^{\frac{x}{2c}}\ , \theta(\eta) = \frac{T-T_\infty}{T_s-T_\infty},\ \emptyset(\eta) = \frac{C-C_\infty}{C_s-C_\infty},\ u = me^{\frac{x}{c}}f'(\eta),$$

$$v = -\sqrt{\frac{vm}{2c}}\, e^{\frac{x}{2c}}\big(f(\eta) + \eta f'(\eta)\big) \tag{6}$$

with $m > 0$ indicating a stretching condition and $m < 0$ suggesting a shrinking state. The stream function expressions are given by

$$u = \psi'(y), v = -\psi'(x) \tag{7}$$

Meanwhile, from equations (1) – (4), the following symbols $u, v, p, \mu, \sigma, \rho, g, \lambda, Re, k, c_p,$ and D_c represent the velocities in both x and y axes, constant pressure, dynamic viscosity, electrical conductance, base fluid density, gravitational acceleration, base fluid's volumetric heat enlargement coefficient, Reynolds number, the thermal conductivity of the fluid, heat at constant pressure, and coefficient of mass diffusivity, respectively. It is vital to note that the additive inverse in equation (5) implies that suction takes place along the path of the stretched surface and the thermal boundary constraint is dependent on the convection transfer process. The primes in equation (6) refer to differentiation concerning the independent variable, η.

3.2. The Regular Approximation Technique

To solve the coupled ordinary differential equation featuring a small parameter ξ, the regular approximation method is applied. The method is particularly valuable when it is challenging or impractical to solve such coupled equations directly probably due to their coupled nature, or complexity. In such a situation, it can be simplified under the assumption that the parameter, $\xi \ll 1$. Thus, the first thing is to ascertain that the differential equations or system of equations governing the problem to be solved have been clearly defined. Thereafter, the equation's tiny perturbation parameter ξ is determined. To arrange the terms for the perturbation analysis, a scaling analysis is performed to find the typical scales in the problem and to ascertain the terms that dominate in different orders of the small parameter, ξ. The next step in the solution step is to carry out an approximate expansion transformation in terms of the powers of the small parameter. ξ followed by a definition of a sequential solution. Usually, such a solution takes the form of

$$p(\eta) = \sum_{n=0}^{\infty} \xi^n\, p_n(\eta) \tag{8}$$

where, the functions to be obtained are denoted by $p_n(\eta)$. To generate a series of sequential equations from Equation (8), the proposed solution is used in the original ODEs. Thereafter, the coefficients of similar orders of ξ are equated to create a set of equations involving the following unknown functions $p_0(\eta)$, $p_1(\eta)$, $p_2(\eta)$, etc. These equations are solved to determine the formulas for the unknown functions. After finding the equations for $p_0(\eta)$, $p_1(\eta)$, $p_2(\eta)$, they are substituted into Equation (8) to obtain the approximate solution of $p(\eta)$. Meanwhile, the integration constants in the generated solutions are found by applying the transformed primary boundary conditions. The rationale behind the choice of the adopted method in this study is primarily driven by its simplicity and effectiveness in analytically resolving the coupled ordinary differential equations. The series method offers a straightforward approach to obtaining solutions with clearly defined convergence properties making it particularly suitable for the specific boundary layer problems addressed in this research. However, while the Keller-Box method may provide numerical solutions with good precision, it often involves more complex discretization and stability considerations which may complicate the analytical process. Also, although the Homotopy Analysis Method (HAM) seems appropriate for certain types of non-linear problems, it is associated with higher computational overhead and requires careful selection of auxiliary parameters which may not be necessary for the present study's objectives. Ultimately, the series method provides a more direct path to achieving the analytical and numerical results and maintains clarity and interpretability of the fluid dynamics involved. The Equation (1) is satisfied as demonstrated below when Equation (7) is introduced into it.

$$\frac{\partial^2\Psi}{\partial x\partial y} + \frac{\partial^2\Psi}{\partial x\partial y}\ = 0 \tag{9}$$

Progressively, Equations (2) to (5) are transmuted into Equations (10) to (13) through the similarity approximation process, application of Equation (6), and solved sequentially:

$$f'''(\eta) + f''(\eta)f(\eta) - Htf'(\eta) + \theta(\eta)G_t = 0 \tag{10}$$

$$\theta''(\eta) + P_o f(\eta)\theta'(\eta) + E_o\theta(\eta) = 0 \tag{11}$$

$$\emptyset''(\eta) + Scf(\eta)\emptyset'(\eta) \tag{12}$$

$$f(0) = k_0,\ f'(0) = 1,\ f'(\infty) = 0,\ \theta(0) = 1,\ \theta(\infty) = 0,\ \emptyset(0) = 1,\ \emptyset(\infty) = 0 \tag{13}$$

Accordingly, the following physical parameters are obtained. $E_o = \frac{2\mu v l}{kU_w\Delta T}$ is the thermal nonequilibrium (Brinkman) parameter with, $\Delta T = (T_w - T_\infty)$, $Ht = \frac{2l\sigma B_o^2}{\rho U_w}$ refers to the magnetic strength parameter, $G_t = \frac{2g\lambda(T_w - T_\infty)}{U_w^2\, R_e^2}$ indicates the threshold thermal Grashoff number, $P_o = \frac{\mu C_p}{k}$ expresses the Prandtl intensity, and $Sc = \frac{v}{D_c}$ specifies the Schmidt factor. In line with [28], let

$$\eta = \Gamma\lambda_o,\ f(\eta) = \lambda_o F(\eta),\ \theta(\eta) = h(\eta),\ \xi = \frac{1}{\lambda_o^2},\ \emptyset(\eta) = \varphi(\eta) \tag{14}$$

Putting equation (14) and its differentials into equations (10) to (13) produce

$$f'''(\eta) + f''(\eta)f(\eta) - \xi Htf'(\eta) + \xi^2 h(\eta)G_t = 0 \tag{15}$$

$$h''(\eta) + p_0 f(\eta)h'(\eta) + \xi E_o h(\eta) = 0 \tag{16}$$

$$\varphi''(\eta) + Scf(\eta)\varphi'(\eta) = 0 \tag{17}$$

$$F(0) = 1,\ F'(0) = \delta,\ F'(\infty) = 0,\ h(0) = 1,\ h(\infty) = 0,\ \varphi(0) = 1,\ \varphi(\infty) = 0 \tag{18}$$

Since $\delta \ll 1$, we define the solutions of equations (15) to (17) as follows.

$$f(\eta) = 1 + \sum_{z=n=1}^{\infty} z\, f_n(\eta) \tag{19}$$

$$h(\eta) = \sum_{z=n=1}^{\infty} (\xi)^z\, h_n(\eta) \tag{20}$$

$$s(\eta) = \sum_{z=n=1}^{\infty} (\xi)^z\, \varphi_n(\eta) \tag{21}$$

Hence, the following equations are obtained by taking the derivatives of equations (19) thrice, and equations (20) to (21) twice with respect to η. The results are substituted into equations (15) to (18) and simplified. Then, the coefficients of equal powers are equated and the following results are obtained.

O(ξ^0):

$$h_0''(\eta) + P_0 h_0'(\eta) = 0;\ h_0(0) = 1, h_0(\infty) = 0 \tag{22}$$

$$\varphi_0''(\eta) + Sc\varphi_0'(\eta) = 0;\ \varphi_0(0) = 1, \varphi_0(\infty) = 0 \tag{23}$$

O(ξ):

$$f_1'''(\eta) + f_1''(\eta) = 0;\ f_1(0) = 0, f_1'(0) = 1, f_1'(\infty) = 0 \tag{24}$$

$$h_1''(\eta) + Ph_1'(\eta) + P_0 f_1(\eta)h_0'(\eta) + E_o h(0) = 0;\ h_1(0) = 0,\ h_1(\infty) = 0 \tag{25}$$

$$\varphi_1''(\eta) + Sc\varphi_1'(\eta) + Scf_1(\eta)\varphi_0'(\eta) = 0;\ \varphi_1(0) = 0,\ \varphi_1(\infty) = 0 \tag{26}$$

O(ξ^2):

$$f_2'''(\eta) + f_2''(\eta) + f_1(\eta)f_1''(\eta) - Htf_1'(\eta) + h_0(\eta)G_t = 0;$$

$$f_2(0) = 0,\ f_2'(0) = 0,\ f_2'(\infty) = 0 \tag{27}$$

Subsequently, equations (22) to (27) are solved analytically and the following results are found. Flow rate (velocity)

$$f'(\eta) = exp - \eta + \varpi(-\eta exp - \eta + exp - \eta - \frac{1}{2}exp - 2\eta - Ht\eta exp - \eta + Htexp - \eta - \frac{G_t(2+P_0)}{{P_0}^2(1+P_0)}exp - (2+P_0)\eta - \frac{1}{2}exp - \eta - Htexp - \eta + \frac{G_t(2+P_0)}{P^2(1+P_0)}exp - \eta) \quad (28)$$

Temperature

$$h(\eta) = exp - P_o\eta + \varpi\left(-P_0\eta exp - P_o\eta - \frac{(P_0)^2}{1+P_0}exp - (1+p_0)\eta + \frac{E_o}{P_0}\eta exp - P_o\eta + \frac{{P_0}^2}{1+P_0}exp - P_o\eta\right) \quad (29)$$

Concentration specie

$$\varphi(\eta) = exp - Sc\eta + \varpi\left(-\mathrm{Sc}\eta exp - Sc\eta - \frac{(\mathrm{Sc})^2}{1+\mathrm{Sc}}exp - (1+Sc)\eta + \frac{(\mathrm{Sc})^2}{1+\mathrm{Sc}}exp - Sc\eta\right) \quad (30)$$

3.3. Physical Quantities

Of utmost importance to the engineering, thermal, and material sciences are skin friction and wall local thermal transfer rate which are defined below.

$$Cf_x = \frac{\tau_w}{\rho U_W^2} = \frac{f''(0)}{\sqrt{2Re_x}} \qquad f''(0) = -1 + \varpi\left(-\frac{1}{2} - Ht + \frac{G_t(2+P_0)^2}{{P_0}^2(1+P_0)} - \frac{G_t(2+P_0)}{{P_0}^2(1+P_0)}\right) \quad (31)$$

$$q_w = -P_o w'(\eta)_{\eta=0} \quad N_{ux} = -k(T_w - T_\infty)\sqrt{\frac{a}{2vc}}\, e^{\frac{x}{2c}} h'(0) \qquad h'(\eta) = -P_o + \varepsilon\left(-p_o + {p_o}^2 + \frac{E_o}{P_o} - \frac{{P_o}^3}{1+P_o}\right) \quad (32)$$

4. Results and Discussion

The analytical solutions are presented in equations (28), (29), (30), (31), and (32) respectively while their numerical solutions are shown in Figs. 2 to 10. However, the effect of pertinent parameters on the velocity, temperature, and concentration distributions are presented in graphical forms with legends followed by detailed analysis. The dimensionless velocity f', temperature h, and concentration φ appear on the vertical axis while the independent variable η is on the horizontal axis of the graphs. The Hartmann number (Ht) quantifies the influence of the strength of a magnetic field on a conducting fluid. An increase in the Hartmann number signifies a stronger magnetic field which enhances the Lorentz force acting on the charged particles in the fluid. This force opposes the fluid motion and creates a damping effect that reduces the velocity of the fluid [3,5] as shown in Fig. 2. This phenomenon is central in the study of MHD since it revolves around the dynamics of electrically conducting fluids in the presence of magnetic fields. A significant application of the parameter is in the design and optimization of cooling systems for nuclear reactors in which liquid metal coolants are subjected to a strong magnetic field for controlling and stabilizing the flow, ensuring efficient heat transmission, and safe operation. Physically, it is primarily associated with MHDs and signifies the relative significance of magnetic forces compared to viscous forces in a conducting fluid. It indicates that the magnetic forces dominate the viscous forces thereby leading to a more streamlined flow that is less influenced by viscosity. Conversely, a low Hartmann number implies that viscous effects are more significant and this causes a more chaotic flow regime. The real-world applications of the Ht are as follows.

- **Electromagnetic Flow Control**: In industries where electrically conductive liquids (such as molten metals) are used, the Hartmann number helps to guide the effectiveness of magnetic fields in controlling the flow and enhancing mixing or stabilizing processes.
- **MHD Power Generation**: In MHD generators, the parameter is crucial for evaluating the effectiveness of the magnetic fields in extracting energy from the conducting fluids. A higher Ht often means a better conversion efficiency.
- **Nuclear Fusion Reactors**: In fusion plasma physics, understanding the behavior of conducting fluids under the influence of a magnetic field is vital for predicting the stability of plasma and confinement conditions.

- Material Processing: The use of magnetic fields in processes such as continuous casting or metal processing could be helpful from the analysis of the Hartmann number, Ht by stabilizing the flow and controlling the temperature distributions.

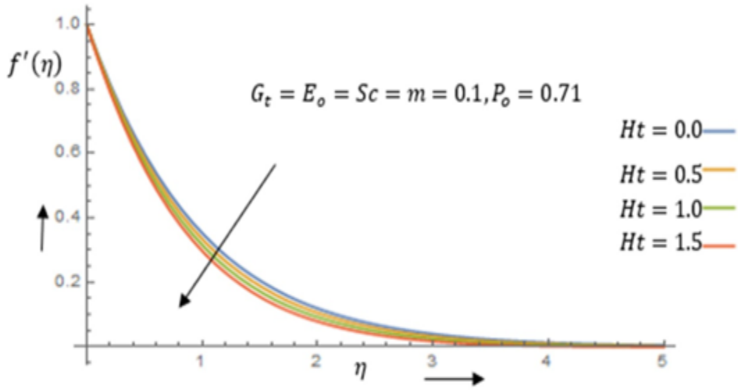

Figure 2. Velocity profile for Ht

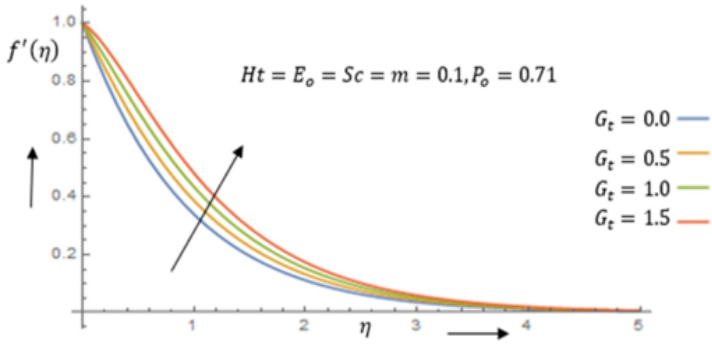

Figure 3. Velocity profile for G_t

Figure 3 displays the effect of the threshold thermal Grashoff number, G_t on the velocity distribution. This parameter (G_t) measures the impact of buoyancy forces resulting from the temperature gradients within a fluid. Its enhancement is an indication of a higher temperature differential between regions of the fluid which in turn amplifies buoyancy forces. These forces induce stronger convective currents and accelerate the fluid's motion and turbulence near the surface thereby increasing its velocity. Thus, this turbulent motion increases skin friction because the turbulent flow has higher energy dissipation and shear stress at the surface which causes more drag [29]. Therefore, by optimizing the value of this parameter, the efficiency of heat dissipation can be enhanced through convective cooling. This phenomenon aids electronic components to maintain safe operating temperatures even under high power loads [30]. Figure 4 interprets the velocity field as a result of variations in the suction parameter (m). An increase in this parameter suppresses the velocity due to the principles of fluid

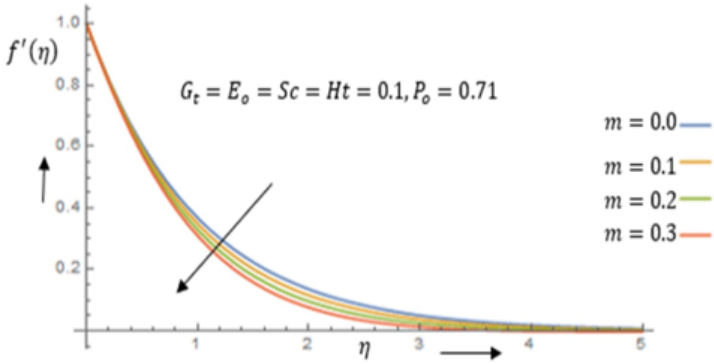

Figure 4. Velocity profile for m

dynamics particularly the Bernoulli equation which states that an increase in the pressure difference (caused by suction) results in a decrease in the fluid velocity. When suction is applied, a higher-pressure gradient across the fluid is created. This gradient causes the fluid to accelerate towards the lower pressure region. However, as the fluid particles are drawn into the suction area, there is a drop in the kinetic energy due to the wall friction and it leads to a decrease in the overall velocity as evident in Fig. 4. This phenomenon is commonly observed in various applications such as the functioning of vacuum pumps and suction devices [31]. The decrease in the kinetic energy of the fluid particles especially in the context of a flow system (such as a pump or an airflow system) can be attributed to several interconnected factors primarily related to the viscous effects, wall friction, and energy transformations within the fluid system.

1. Viscous Drag and Wall Friction

When the fluid particles move through a conduit or any other physical boundary they are subjected to viscous forces. Meanwhile, viscosity measures a fluid's resistance to deformation and flow. As the fluid comes into contact with the walls of the area of the suction, the following occurs.

- **Velocity Gradient:** Fluid particles in direct contact with the wall adhere to it (due to the no-slip condition). This means that they have zero velocity relative to the wall. As they move away from the wall, the velocity increases so as to match the flow. This creates a velocity gradient which leads to a shear stress in the fluid [32].
- **Energy Dissipation:** The shear stress induces frictional forces between the successive layers of the fluid (viscous drag). As the fluid layers interact, energy is transferred and also lost to heat due to the frictional interactions which leads to energy dissipation. This energy loss manifests as a decrease in the kinetic energy of the fluid particles as they approach the wall [33].

2. Flow Constriction and Acceleration Changes

As the fluid is drawn into the area of the suction, the geometry often changes and can impact flow velocity in the following ways:

- **Converging Flow:** If the suction area has a narrowing section (for example, in a venturi effect or the throat of a nozzle), the fluid must accelerate to pass through the constricted area. Initially, as the fluid enters the suction area, it may slow down due to the resistance from the surrounding walls and create the required velocity only after some acceleration. This initial slowing down can lead to a momentary decrease in the kinetic energy [34].
- **Bernoulli's Principle**: According to Bernoulli's principle, an increase in the fluid velocity creates a decrease in the pressure and kinetic energy of a streamlined flow. When particles enter a region of higher resistance (like a suction area) the pressure can increase momentarily to cause energy redistribution where part of the kinetic energy may be converted into potential energy thereby leading to a decreased kinetic energy [35].

3. Turbulence and Flow Separation

As the fluid moves toward the suction area, it may encounter obstacles or changes in the flow conditions that induce turbulence.

- **Turbulent Flow:** In turbulent flow, the formation of eddies and vortices can lead to chaotic changes in the energy distribution. Due to these turbulent interactions, some kinetic energy is transformed into thermal energy which also produces losses in the kinetic energy of the fluid particles [36].
- **Flow Separation**: If the geometry of the suction area is such that it causes flow separation, then it can lead to an adverse pressure gradient which will further detract from the kinetic energy of the fluid particles.

In summary, the decrease in the kinetic energy of the fluid particles being drawn into the suction area is primarily caused by the:

- viscous drag and wall friction that dissipate energy into heat.

- changes in the velocity due to the flow constriction which leads to an initial acceleration and overall energy loss.
- turbulent interactions that transform kinetic energy into thermal energy.
- flow separation and adverse pressure gradients that further hinder the kinetic energy of the approaching fluid particles [37].

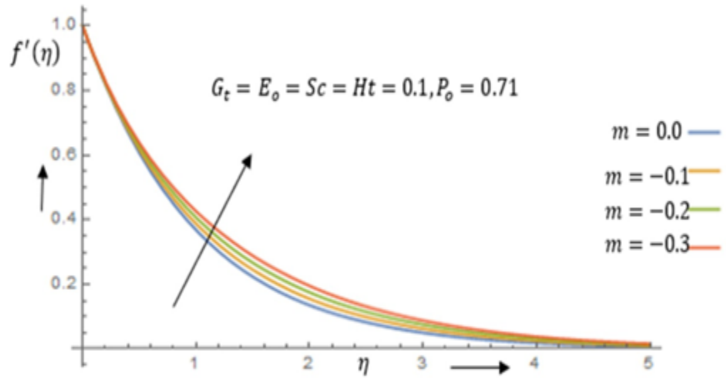

Figure 5. Velocity profile for $-m$

However, in fluid dynamics, a decrease in suction leads to an increase in velocity because of the inverse relationship between pressure and velocity described by the Bernoulli equation. When suction is reduced, the pressure gradient across the fluid reduces. This produces a lower pressure difference and causes less acceleration of the fluid particles towards the suction area which allows them to retain more of their kinetic energy. As a result of this, the fluid velocity increases because of the lower pressure drop which means that less energy is lost to overcome the pressure difference. Hence, this leads to a faster flow as shown in Fig. 5. This principle is applicable in various scenarios such as airflow in ducts and fluid movement in pipes.

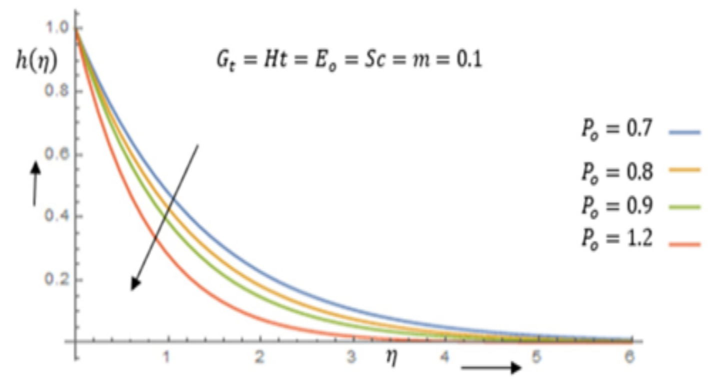

Figure 6. Temperature distribution for P_o

The distribution effect of the Prandtl number (P_o) on the temperature is outlined in Figure 6. An increase in this number signifies that the fluid has greater momentum diffusivity than thermal diffusivity. This means that the fluid's ability to transport momentum (due to viscosity) is more effective than its ability to conduct heat. Consequently, as the Prandtl number increases, the thermal boundary layer (the region where the temperature gradients are significant) becomes thinner relative to the velocity boundary layer where momentum transfer occurs. In practical terms, this implies that as the fluid flows with momentum effectively, its capacity to redistribute the thermal energy is limited. Thus, less heat is transferred away from the hot surfaces, leading to a lower temperature gradient near the surface and ultimately a decrease in the overall temperature of the fluid [17, 44]. From the physical perspective, the implications of a higher Prandtl number on the flow dynamics are significant. The greater resistance to thermal changes can lead to a more stable thermal profile, meaning the fluid retains its heat for longer while flowing. This behavior can create regions of localized heating as the energy supplied to the fluid is not dissipated rapidly resulting in a more uniform temperature distribution throughout the fluid. In applications to thermal management and engineering systems, the choice of fluids with high Prandtl numbers can be advantageous for achieving stable temperature profiles and reducing heat loss thereby enhancing the efficiency of cooling or heating processes. Understanding the interplay between the Prandtl number, temperature distribution, and flow characteristics is essential for optimizing thermal performance in various industrial applications. Scientifically, this phenomenon is essential for the heat transfer processes in various applications such as the cooling of electronic components where a high Prandtl number would slow down the thermal dissipation required for different cooling strategies. From the physical perspective, engineers leverage this knowledge to optimize the designing of heat exchangers, HVAC systems, and thermal insulation to efficiently manage heat transfer rates and maintain the desired operating temperatures in industrial processes and technological applications [38].

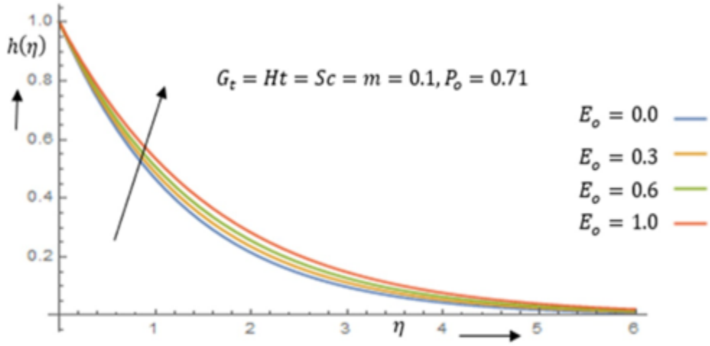

Figure 7. Temperature distribution for E_o

In terms of the physical meaning, the Brinkman number (E_o) is a dimensionless number that characterizes the relative importance of viscous heating to conduction in a fluid flow. An increase in the parameter indicates that the viscous dissipation or conversion of mechanical energy into thermal energy due to the viscosity of the fluid becomes more significant relative to heat conduction. As the viscous forces in the fluid generate more heat as the fluid flows, the overall temperature of the fluid increases [26] as portrayed in Figure 7. This effect is particularly pronounced in areas where the viscous heating is substantial such as in high-temperature applications or flows with high shear rates that lead to a warmer fluid temperature as the energy input from the mechanical work is transformed into thermal energy. Practically, this knowledge is important for enhancing the performance of renewable energy systems such as solar thermal collectors by leveraging a higher Brinkman number (E_o) to achieve higher thermal efficiencies [39]. From a physical perspective, the implications of increasing E_o are critical for understanding the flow behavior in various engineering applications. For instance, in processes involving high shear rates such as those found in polymer processing or certain chemical reactions, enhanced viscous heating can lead to a localized hot spot within the fluid. This leads to a spatially non-uniform temperature distribution which can affect the reaction rates, material properties, and overall system efficiency. Moreover, the increase in temperature can alter the properties of the fluid such as viscosity which impacts the flow dynamics. Therefore, when designing systems where viscous heating is a concern such as in heat exchangers or reactors, it is essential to consider the Brinkman number to ensure optimal thermal management and flow stability. Thus, understanding the balance between viscous heating and heat dissipation is crucial for achieving the desired thermal performance in several applications. Thus, the Brinkman number is applied to the following areas.

- **Heat Exchangers**: In systems where fluids experience significant viscous heating such as in high-speed heat exchangers, the Brinkman number (E_o) helps in its design to optimize heat transfer and thermal performance.
- **Polymer Processing**: During the processing of polymers, the viscosity and flow characteristics can lead to significant heating. Understanding this parameter (E_o) can help to control overheating to avoid the thermal degradation of materials.
- **Geothermal Systems**: In geothermal energy extraction, this parameter (E_o) helps in the assessment of heat transfer efficiency in high-viscosity fluids impacting the design and performance of geothermal systems.
- **Chemical Reactions**: Processes that involve exothermic reactions in viscous fluids indicate the importance of viscous heating which aids in the designing of reactors to ensure safety.

Figure 8 shows the effect of the suction parameter on the temperature field. An increase in suction leads to a decrease in temperature due to the principles of thermodynamics particularly the adiabatic cooling process [5]. When suction is applied, it causes a rapid decrease in pressure within the fluid. As the fluid expands into the lower pressure area created by the suction, it does so without the addition of external heat (adiabatically). This expansion causes the fluid molecules to spread out thereby opposing the surrounding pressure which later reduces their kinetic energy.

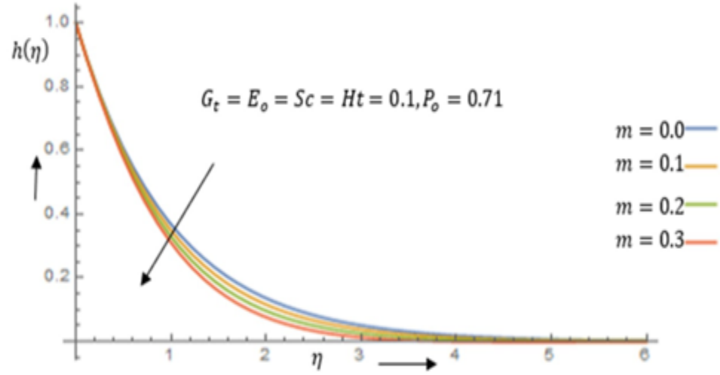

Figure 8. Temperature distribution for m

Since temperature is a measure of the average kinetic energy of the molecules, this decrease in kinetic energy causes a corresponding drop in the temperature. This effect is commonly observed in devices such as refrigerators and air conditioners where increased suction is used to cool the refrigerant.

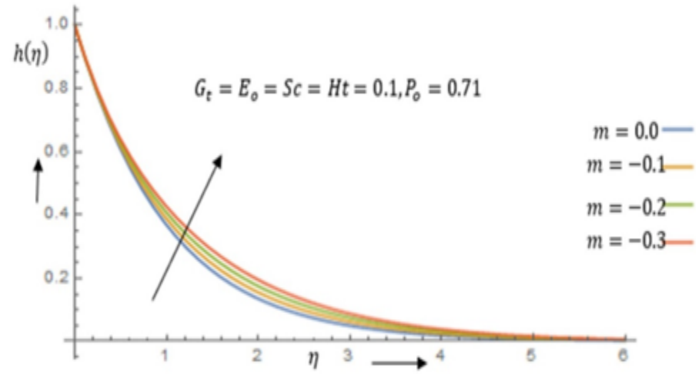

Figure 9. Temperature distribution for $-m$

A decrease in suction leads to an increase in temperature due to the principles of thermodynamics and the behavior of gases under compression. When suction is reduced, the pressure within the fluid increases. As the fluid is compressed, the molecules are brought closer thereby increasing their collisions and kinetic energy. Thus, this increase in the kinetic energy produces a temperature rise which is illustrated in Fig. 9. This process is known as adiabatic heating. It refers to a situation where the work done on the fluid during compression translates into increased thermal energy. This principle is utilized in various applications such as heat pumps and compressors where decreasing suction (or increasing pressure) raises the temperature of the working fluid.

An upsurge in the Schmidt number (Sc) indicates that the diffusivity of momentum (viscosity) relative to the diffusivity of mass (concentration) is higher. This means that momentum is transferred more readily than mass within the fluid. Consequently, when Sc appreciates, the mass transfer rate decreases because viscous forces dominate over molecular diffusion thereby resulting in a slower mixing and dispersion of the concentration field which is shown in Figure 10. Thus, the concentration decreases as the Schmidt number rises [40]. This effect is significant in some areas of applications such as the chemical engineering processes, environmental fluid dynamics, and biological systems where transporting substances such as pollutants, nutrients, or chemical reactants is key. With the knowledge of this relationship, scientists and engineers can optimize the mixing strategies to design efficient reactors and model pollutant dispersion in natural water bodies or industrial effluents. Practical applications include wastewater treatment whereby controlling the Schmidt number influences the efficiency of processes such as biological nutrient removal or chemical oxidation by adjusting the mixing regimes or reactor configurations to enhance mass transfer rates. However, due to the importance of this study, the effects of some pertinent parameters such as the threshold thermal Grashoff (G_t) and Brinkmann numbers (E_o)

on skin friction and Prandtl number P_o on the wall heat transfer have been tabulated and shown in Tables 1 and 2, respectively. Both tables contain the numerical values of some thermophysical parameters that have been varied to find their effect on skin friction and Nusselt number. However, understanding the trends in both tables would be helpful in the energy optimization, thermal management, and polymer extrusion processes.

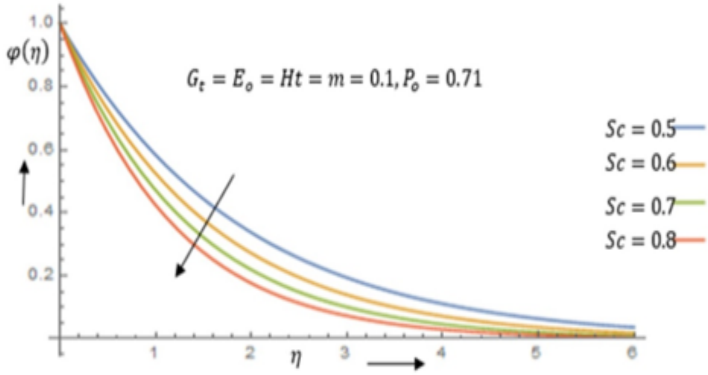

Figure 10. Concentration distribution for Sc

Table 1. The Influence of G_t and Ht on Skin Friction.

Threshold thermal Grashoff Number G_t	Hartmann Number, Ht	Prandtl Number, P_o	Brinkman Number, E_o	Akhar et al. [41]RK $-f''(0)$	Akhar et al. [41]NFD $-f''(0)$	Skin Friction, $-f''(0)$ Present Result
0.5	0.0	0.71	0.0	0.80274	0.80275	0.78120
1.0	0.0	0.71	0.5	0.61617	0.61612	0.51241
0.5	1.0	0.71	0.0	1.22381	1.22388	1.10000
1.0	1.0	0.71	0.5	1.04349	1.04352	1.15000

The threshold thermal Grashoff number (G_t) signifies the ratio of buoyancy forces to viscous forces in a fluid flow affected by temperature gradients. An increase in this number indicates a stronger buoyancy relative to viscous forces thus leading to an enhanced fluid motion and turbulence near a wall surface. This turbulent motion increases skin friction because turbulent flow has higher energy dissipation and shear stress at the surface and causes greater drag. Conversely, the Hartmann number Ht represents the ratio of electromagnetic forces (Lorentz forces) to viscous forces in MHD flows which are influenced by a magnetic field. An improvement in this parameter (Ht) strengthens the Lorentz forces and suppresses the fluid motion and turbulence near the surface due to the magnetic damping effect. This suppression reduces the velocity gradients and turbulence intensity at the surface and causes a decline in skin friction [3]. Meanwhile, skin friction is crucial for aerospace, production processes, automobiles, and geophysical science. With this understanding, controlling aerodynamics becomes essential for optimizing aircraft and vehicle designs to reduce drag and improve efficiency. In geophysics, it affects the behavior of fluids in geological formations and oceans and influences natural processes including convection and climate dynamics.

Table 2. The Influence of Prandtl, P_o and Brinkman numbers, E_o on the wall heat transmission, $h'(0)$.

Hartmann Number, Ht	Stretching Sheet parametric Condition, m	Prandtl Number, P_o	Brinkman Number, E_o	Bidin and Nazar [42]	Ishak [43]	Nusselt Number, $-h'(0)$
0.0	0.1	1.00	3.0	0.9547	0.9548	0.7500
0.0	0.1	2.00	3.0	1.4714	1.4715	1.9167
0.0	0.1	3.00	3.0	1.8691	1.8691	2.3750

An increase in the Prandtl number corresponds to a higher ratio of momentum diffusivity (kinematic viscosity) to thermal diffusivity in a fluid and it's indicative of the fact that the thermal conduction occurs more readily than momentum diffusion. This characteristic enhances the efficiency of convective heat transfer processes since the thermal energy can move more effectively through the fluid. Understanding and controlling convective heat transfer via the Nusselt number is essential for achieving efficient energy utilization, reducing operational costs, and improving the performance and durability of machinery and equipment. Scientifically, the rate of heat transport provides a quantitative measure of convective heat transfer efficiency, aiding in developing advanced heat transfer models, climate control systems, and thermal insulation materials.

4. Conclusions

The examination of the boundary layer thickness and temperature transfer effects in a viscous fluid flow with different Hartmann and thermal nonequilibrium effects over an exponentially stretching/shrinking plate has been analyzed in the present study. Thus, the following points are significant:

1. An increase in the suction parameter m leads to a decline in the velocity and temperature while a decrease in the parameter shows a reversed trend in the velocity and temperature distributions.
2. The enhancement of the Hartman number Ht initiate a fall in the velocity and skin friction.
3. As the Brinkman number E_o improves, the thermal boundary layer and Nusselt number $h'(0)$ are enhanced.
4. An increase in the Schmidt number Sc suppresses the concentration distribution.
5. An increase in the Prandtl number P_o reduces the thermal boundary layer thickness and improves the rate of heat transfer $h'(0)$.

The novel findings of the present study stand out due to the incorporation of the effects of thermal non-equilibrium and viscous heating simultaneously within the context of fluid flow over an exponentially stretching/attenuating sheet. Unlike many previous works that focus solely on thermal equilibrium conditions or simplified geometries, this research provides a comprehensive exploration of how the aforementioned pertinent parameters influence the boundary layer dynamics, velocity, temperature, and concentration distributions.

Table 3. A Comparison highlighting the similarities with existing studies.

	Author(s)	Parameters	Similarities	Present Study
1.	Shuguang et al., [47].	Hartmann Number, Ht.	As the Lorentz forces become stronger for higher Hartmann numbers, the velocity decreases.	The enhancement of the Hartman number, Ht leads to a reduction in the velocity.
2.	Shuguang et al., [47].	Schmidt Number, Sc.	An upsurge in the value of the Schmidt number creates a decline in the concentration field.	An increase in the Schmidt number, Sc improves the concentration distribution.
3.	Y. Dharmendar Reddy et al., [45].	Prandtl Number, Po.	An increase in the Prandtl number Po creates a diminution in the thermal boundary layer, which outcomes in a decrease in the temperature profile.	As the Prandtl number rises, the temperature decreases.
4.	Akhar et al., [41]	Thermal Grashoff Number, G_t.	Increasing the thermal Grashoff number G_t significantly lowers skin friction.	Skin friction is significantly reduced by raising the thermal Grashoff number. G_t.
5.	Krishnamurthy et al., [46].	Hartmann Number, Ht.	The strength of the magnetic field similarly increases with a higher Hartmann number M. In the stretched nanofluid sheet, it increases the thickness of the momentum boundary layer thereby preventing the flow.	The strength of the magnetic field increases as the Hartmann number Ht rises. In addition to the obstruction of the flow, it thickens the momentum barrier layer in the stretching nanofluid sheet.

A notable finding is an observation that the distributions of skin friction for the effects of thermal Grashoff number at two different values of the Hartmann (MHD) number, i.e., $Ht = 0.0$ which indicates an electrically non-conducting case and $Ht = 1.0$ meaning an electrically conducting case which is shown in Table 1 indicated that the magnitude of skin friction is significantly elevated with the increasing magnetic field at different values of the thermal Grashoff number i.e., $G_t = 0.5$ and 1.0. Furthermore, the work uniquely demonstrates that the thermal non-equilibrium parameter enhances temperature while an increased thermal Grashoff number leads to improved skin friction. This highlights the intricate dependencies that are often overlooked in conventional analyses.

Another novel aspect is the dual-method approach of solution involving the combination of the analytical series technique and a robust numerical scheme via the MATHEMATICA, with a detailed analysis of the results obtained. In comparison to the literature, the results of the present study in the graphical and tabular presentations of varying parametric values are exceptionally detailed. By bridging the gaps in understanding the interplay between thermal and magnetic effects, this research contributes to a richer, and multi-dimensional perspective to the field of boundary layer theory.
However, in terms of this study's differences compared to similar parameters in the literature, it was noted that:

1. an increase in the Prandtl number reduces the diminution of the thermal boundary layer which brings about a decrease in the temperature [45]. Thus, it improves the rate of heat transfer.
2. the Brinkmann number is an increasing function of the temperature distribution while in [40], it is a decreasing function of the velocity field.
3. the fluid velocity decreases with increasing values of the Hartmann number Ht (magnetic effect), while [44] reported an increase in the velocity.

Also, a comparison of the similarities of the results in the present study with existing studies in the literature has been tabulated and shown in Table 3. It would be beneficial to explore the effects of varying fluid properties such as non-Newtonian fluid characteristics on the boundary layer dynamics and thermal distributions in similar flow configurations.

Acknowledgments

The authors express their appreciation to Professor Emeka Amos for his constructive input towards the success of this work.

Authors' Contributions

UU conceived and designed the research study. UU, EE, and OI contribute to the theoretical framework of the research through the provision of critical intellectual input throughout the research process. UU obtained the solution of the transformed mathematical model. UU, EE, and OI carried out the result analysis, and interpretation of results, and participated in the revision and formatting of the research manuscript. UU, EE, and OI re-checked the article not only for spelling and grammatical errors but also for intellectual content. All the authors read and approved the final manuscript.

Competing Interests

The authors state that no competing interests are in existence.

References

[1] B. C. Sakiadis, "Boundary layer behavior on continuous solid surfaces: I. Boundary layer equations for two-dimensional and axisymmetric flow", American Institute of Chemical Engineers (AIChE J.), vol. 7, pp. 26-28, 1961. https://doi:10.1002/aic.690070108
[2] V. Poply, P. Singh, and A. K. Yadav, "A study of Temperature-dependent fluid properties on MHD free stream flow and heat transfer over a non-linearly stretching sheet", Proc Eng, vol. 127, pp. 391-397, 2015. https://doi:10.1016/j.proeng.2015.11.386
[3] K. V. Prasad, K. Vajravelu, and P. S. Datti, "The effects of variable fluid properties on the hydro-magnetic flow and heat transfer over a non-linearly stretching sheet", International journal of thermal science, 49(3): 603-610, (2010). https://doi:10.1016/j.ijthermalsci.2009.08.005
[4] R. L. V. D. Renuka, T. Poornima, R. N. Bhaskar, and S. Venkataraman, "Radiation and mass transfer effects on MHD boundary layer flow due to an exponentially stretching sheet with a heat source", International Journal of Engineering Innovative Technology, vol. 3, pp. 33-39, 2014.

[5] S. Mukhopadhyay, "Slip effects on MHD boundary layer flow over an exponentially stretching sheet with suction/blowing and thermal radiation", Ain Shams Engineering Journal, vol. 4, pp. 485-491, 2012. https://doi: 10.1016/jasej.2012.10.007
[6] E. Mabood, W. A. Khan, and A. I. Md Ismail, "MHD flow over exponential radiating stretching sheet using Homotopy Analysis Method" Journal of King Saud University Engineering Science, vol. 29, pp. 68-74, 2017.
[7] T. Poornima, and R. N. Bhask, "Radiation effects on MHD free convective boundary layer flow of nanofluids over a nonlinear stretching sheet", Advances in Applied Science Research, vol. 4, pp. 190-202, 2013.
[8] W. A. Khan, O. D. Makinde, and Z. H. Khan, "Non-aligned MHD stagnation point flow of variable viscosity nanofluids past a stretching sheet with radiative heat", International Journal of Heat and Mass Transfer, vol. 96, pp. 525-534, 2016. https://doi: 10.1016/j..ijheatmasstransfer.2016.01.052.
[9] N. Bachok, A. Ishak, and I. Pop, "Boundary layer stagnation-point flow and heat transfer over an exponentially stretching/shrinking sheet in a nanofluid", International Journal of Heat and Mass Transfer, vol. 55, pp. 8122-8128, 2012. https://doi: 10.1016/j.ijheatmasstransfer.2012.08.051
[10] M. Y. Malik, M. Naseer, S. Nadeem, and A. Rehman, "The boundary layer flow of Casson nanofluid over a vertical exponentially stretching cylinder", Applied Nanoscience, vol. 4, pp. 869-873, 2014. https://doi: 10.1007/s13204-013-0267.0.
[11] M. R. Eid, "Chemical reaction effect on MHD boundary-layer flow of two-phase nanofluid model over an exponentially stretching sheet with a heat generation", Journal of Molecular Liquids, vol. 220, pp. 718-725, 2016. https://doi: 10.1016/j.molliq.2016.05.005.
[12] T. Gangaiah, N. Saidulu, and L. A. Venkata, "Magnetohydrodynamic flow of nanofluid over an exponentially stretching sheet in the presence of viscous dissipation and chemical reaction", Journal of Nanofluids, vol. 7, pp. 439-4448, 2018. https://doi: 10.1166/jon.2018.1465.
[13] M. Abel, S. Mahantesh, M. Nandeppanavar, and V. Basanagouda, "Effects of variable viscosity, buoyancy, and variable thermal conductivity on mixed convection heat transfer due to an exponentially stretching surface with magnetic field", Proceedings of the National Academy of Sciences, India Section A: Physical Sciences, vol. 87, pp. 247-256, 2017. https://doi: 10.1007/s40010-016-0338-1.
[14] M. A. Yousif, I. H. Farhan, T. Abbas, and R. Ellahi, "Numerical study of momentum and heat transfer of MHD Carreau nanofluid over an exponentially stretched plate with internal heat source/sink and radiation", Heat Transfer Research, vol. 50(7), pp. 649-658, 2019. https://doi: 10.1615/HeatransRes.208025568
[15] R. Ellahi, A. Zeeshan, F. Hussain, and T. Abbas, "Thermally charged MHD Bi-phase flow coatings with non-Newtonian nanofluid and Hafnium particles along slippery walls", Coatings, vol. 9, No. 5, pp. 300, 2019. https://doi: 10.3390/coatings9050300.
[16] Z. Ahmed, S. Nadeem, S. Saleem, and R. Ellahi, "Numerical study of unsteady flow and heat transfer CNT-based MHD nanofluid with variable viscosity over a permeable shrinking surface", International Journal of Numerical Methods for heat and fluid flow, vol. 29(12), pp. 4607-4623, 2019. https://doi: 10.1108/HFF-04-2019-0346.
[17] M. Naseer, M. Y. Malik, S. Nadeem, and A. Rehman, "The boundary layer flow of hyperbolic tangent fluid over a vertical exponentially stretching cylinder", Alexandra Engineering Journal, vol. 53, pp. 747-750, 2014.
[18] R. R. Rangi, and N. Ahmad, "Boundary layer flow past over the stretching cylinder with variable thermal conductivity", Applied Mathematics, vol. 3, p. 205-209, 2012.
[19] M. S. Abel, and N. Mathesha, "Heat transfer in MHD viscoelastic fluid flow over a stretching sheet with variable thermal conductivity and non-uniform heat source", Applied Mathematical Modeling, vol. 32, pp. 1965-1983, 1997.
[20] A. Öztürk, F. Sönme, and A. Kabakuş, "Determination of optimum parameters using different nanofluids in heat pipe heat exchangers with response surface method", Chemical Engineering Communications, vol. 211, No. 5, pp. 725-735, 2023. https://doi.org/10.1080/00986445.2023.2289146
[21] A. Öztürk, F. Sönme, and A. Kabakuş, "Optimization of Parameters Affecting the Thermal Efficiency in Heat Pipes Using Different Nanofluids with Taguchi Method", Yüzüncü Yıl University Institute of Science and Technology Journal, vol. 28, No. 3, pp. 1081-1090, 2023. https://doi.org/10.10.53433/yyufbed.1242697
[22] S. Mukhopadhyay, "Analysis of boundary layer flow over a porous nonlinearly stretching sheet with partial slip at the boundary", Alexandria Engineering Journal, vol. 52, pp. 563–569, 2013. http://dx.doi.org/10.1016/j.aej.2013.07.004

[23] Ul. H. Rizwan, Z. Zeeshan, S. S. Syed, " Existence of dual solution for MHD boundary layer flow over a stretching/shrinking surface in the presence of thermal radiation and porous media: KKL nanofluid model", Heliyon, vol. 9(11), e20923, 2023.
[24] B. Nagaraju, N. Kishan, J. V. Tawade, P. Meenapandi, B. Abdullaeva, M. Waqas, M. Gupta, N. Batool, and F. Ahmad, "Analysis of boundary layer flow of a Jeffrey fluid over a stretching or shrinking sheet immersed in a porous medium", Partial Differential Equations in Applied Mathematics, vol. 12, 100951, 2024. https://doi.org/10.1016/j.padiff.2024.100951
[25] R. S. Vidya, P. B. Mallikarjun, and A. J. Chamkha, "Analysis of MHD boundary layer flow of a viscous fluid past a stretching sheet employing the Legendre wavelet method", International Journal of Ambient Energy, vol. 45(1). Article: 2310629, 2024. https://doi.org/10.1080/01430750.2024.2310629
[26] M. K. Joseph, P. Ayuba , And A. S. Magaj, "Effect of Brinkman number and magnetic field on laminar convection in a vertical plate channel", Science World Journal, vol. 12(4), pp. 58-62, 2017.
[27] I. Buongiorno, "Convective transport in nanofluids", Journal of Heat Transfer, vol. 128, pp. 240-250, 2006.
[28] A. R. Bestman, "The boundary layer flow past a semi-infinite heated porous plate for two-components plasma", Astrophysics and Space Science, vol. 173, pp. 93-100, 1990.
[29] F. P. Incropera, and D. P. DeWitt, Fundamentals of Heat and Mass Transfer, 7th Edition., Wiley, 2017.
[30] A. Bejan, Convection Heat Transfer, 4th edition, John Wiley & Sons, 2013.
[31] B. R. Munson, A. T. Rothmayer, and T. H. Okiishi, Fundamentals of Fluid Mechanics, 7th Edition, John Wiley & Sons, 2013.
[32] S. B. Pope, Turbulent Flows, Cambridge University Press, 2000.
[33] T F. Laadhari, "Reynolds number effect on the dissipation function in wall-bounded flows", Physics of Fluids, vol. 19(3), 038101, 2007. https://doi.org/10.1063/1.2711480
[34] J. P. Monty, N. Hutchins, H. C. H. NG, I. Marusic and M. S. Chong, "A comparison of turbulent pipe, channel, and boundary layer flows", Journal of Fluid Mechanics, vol. 632, pp 431-442, 2099. https://doi:10.1017/S0022112009007423
[35] S. B. Pope, Turbulent Flows, Cambridge University Press, (Cornell University), 2000.
[36] D. Modesti, and S. Pirozzoli, "Reynolds and Mach number effects in compressible turbulent channel flow", International Journal of Heat and Fluid flows, vol. 39. Pp. 33-49, 2016.https://doi:10.1016/j.ijheatfluidflow.2016.01.007
[37] H. Schlichting, and K. Gersten, Boundary-Layer Theory, 8th Revised and Enlarged edition, Springer, McGraw Hill, 2000. DOI 10.1007/978-3-642-85829-1
[38] Y. A. Çengel, and A. J. Ghajar, Heat and Mass Transfer: Fundamentals and Applications, 5th Edition, McGraw-Hill, 2019.
[39] F. P. Incropera, and D. P. DeWitt, Fundamentals of Heat and Mass Transfer, 7th edition, Wiley, 2017.
[40] M. Ramzan, Z. Un Nisa, M. Ahmad, and M. Nazar, "Flow of Brinkman fluid with heat generation and chemical reaction", Hindawi Complexity, vol. 2021, pp. 1-11, Article ID 5757991, 11 pages https://doi.org/10.1155/2021/5757991
[41] N. S. Akhar, D. Tripathi, Z. H. Khan, and O. A. Beg, "A numerical study of magnetohydrodynamic transport of nanofluids over a vertical stretching sheet with exponential temperature-dependent viscosity and buoyancy effects, Chemical Physics Letters, 2016, https://doi.org/101016/j.cplett.2016.08.043
[42] B. Bidin, and R. Nazar, "Numerical solution of the boundary layer flow over an exponentially stretching sheet with thermal radiation", European Journal of Scientific Research, vol 33(4), pp. 710-717, 2009.
[43] A. Ishak, "MHD boundary layer flow due to an exponentially stretching sheet with radiation effect", Sain Malaysiana, vol. 40, pp. 391-395, 2011.
[44] S. R. Sherı, A. K. Suram1, and P. Modulgua, "Heat and Mass Transfer Effects On MHD Natural Convection Flow Past An Infinite Inclined Plate With Ramped Temperature", J. KSIAM, Vol. 20(4), pp. 355–374, 2016. http://dx.doi.org/10.12941/jksiam.2016.20.355
[45] Y. Dharmendar Reddy, B. Shankar Goud, Kottakkaran Sooppy Nisar, B. Alshahrani, M. Mahmoud, C. Park, "Heat absorption/generation effect on MHD heat transfer fluid flow along a stretching cylinder with a porous medium", Alexandria Engineering Journal, Vol. 64, pp. 659-666, 2023. https://doi.org/10.1016/j.aej.2022.08.049
[46] M. R. Krishnamurthy, B. C. Prasannakumara, B. J. Gireesha, and R. S. R. Gorla, R, "Effect of viscous dissipation on hydromagnetic fluid flow and heat transfer of nanofluid over an exponentially stretching sheet with fluid-particle suspension", Cogent Mathematics, Vol. 2(1), pp. 1-18, 2015. https://doi.org/10.1080/23311835.2015.1050973

[47] L. Shuguang, K. Raghunath, A. Alfaleh, A. et al. "Effects of activation energy and chemical reaction on unsteady MHD dissipative Darcy–Forchheimer squeezed flow of Casson fluid over horizontal channel", Sci Rep, Vo. 13, 2666, 2023. https://doi.org/10.1038/s41598-023-29702-w